

Abrupt bifurcation to chaotic scattering with discontinuous change in fractal dimension

Ying-Cheng Lai

Department of Mathematics and Department of Electrical Engineering, Center for Systems Science and Engineering Research,
Arizona State University, Tempe, Arizona 85287

(Received 12 August 1999)

One of the major routes to chaotic scattering is through an *abrupt* bifurcation by which a nonattracting chaotic saddle is created as a system parameter changes through a critical value. In a previously investigated case, however, the fractal dimension of the set of singularities in the scattering function changes continuously through the bifurcation. We describe a type of abrupt bifurcation to chaotic scattering where this physically relevant dimension changes *discontinuously* at the bifurcation. The bifurcation is illustrated using a class of open Hamiltonian systems consisting of Morse potential hills. [S1063-651X(99)51112-4]

PACS number(s): 05.45.Ac

Chaotic scattering [1–9] is a manifestation of transient chaos [10–12] in open physical systems. What is usually measured in a scattering experiment is scattering functions, i.e., plots of some output variables after the scattering versus some input variables before the scattering. The scattering is chaotic when such a function contains a set of an uncountably infinite number of singularities. The output of the system then depends sensitively on the input because, a small change in the input variable chosen in the vicinity of a singularity can cause a large change in the output. This is the hallmark of chaos. Despite unboundedness of scattering trajectories both in the physical space and in the phase space, the dynamical invariant set responsible for chaotic scattering is still bounded. These are *nonattracting chaotic saddles* in the scattering region, where the interaction of the particle with the scatterers occurs. The set of singularities in the scattering function is in fact the set of interacting points between the stable manifold of the chaotic saddle and the line from which scattering particles are initiated [2,11]. Chaotic scattering has been identified in a variety of physical contexts such as atomic physics [3], astrophysics [4], fluid dynamics [5], chemical reaction [6], electron transport in mesoscopic systems [7], and even quantum cosmology [8].

An important problem in the study of chaotic scattering is to understand how it arises as a system parameter changes. A major route to chaotic scattering is the *abrupt* bifurcation route in which a chaotic saddle is suddenly created. This route to chaotic scattering was described and analyzed in Ref. [9] by using a representative two-degree-of-freedom Hamiltonian system with the following potential function: $V(x,y) = x^2y^2e^{-(x^2+y^2)}$. This potential is appreciable in the scattering region near the origin $(x,y) = (0,0)$ but it is negligible at large distances from the origin. There are four identical potential hills located at $(x,y) = (\pm 1, \pm 1)$. When the particle energy E is greater than V_m , the height of each potential hill, the dynamics is smooth because a scattering particle can simply penetrate each hill and exit to infinity. However, when E is smaller than V_m , a particle can be trapped in the scattering region and the dynamics can be complicated. It was argued in Ref. [9] that a chaotic saddle containing an infinite number of unstable periodic orbits is created when E is decreased through V_m . Physically, these

unstable periodic orbits correspond to particle trajectories bouncing permanently between the potential hills. It was also argued that the fractal dimension of the set of singularities in the scattering function starts to increase from zero as E is decreased from V_m in the following manner: $D_0(E) \sim 1/\ln[(V_m - E)^{-1}]$, where D_0 is the box-counting dimension. A feature to notice in this route to chaotic scattering is that before the bifurcation ($E > V_m$), $D_0(E = V_m + 0) = 0$, while after the bifurcation ($E < V_m$), we have $\lim_{E \rightarrow V_m - 0} D_0(E) = 0$. Thus, although the bifurcation at V_m is called *abrupt*, the fractal dimension $D_0(E)$ is still continuous at the bifurcation.

In this Rapid Communication, we describe a different type of abrupt bifurcation to chaotic scattering in two-degree-of-freedom open Hamiltonian systems: $H(\mathbf{p}, \mathbf{q}) = \mathbf{p}^2/2m + V(\mathbf{q})$, where m is the particle mass, $\mathbf{q} = (x, y)$ and $\mathbf{p} = (p_x, p_y)$ are the conjugate coordinate and momentum vectors, respectively, and $V(\mathbf{q})$ is a potential function. Let the particle energy E be the bifurcation parameter and E_c be the bifurcation point. Before the bifurcation (say, $E < E_c$), there exists a bounded chaotic region in the phase space surrounded by classically forbidden potential barriers. The bounded chaos is typically developed through the destruction of a hierarchy of Kol'mogorov-Arnol'd-Moser (KAM) tori. Particles from outside cannot enter this bounded chaotic region so that the scattering dynamics is regular. At E_c , the barriers disappear, and the bounded Hamiltonian chaos becomes transient, allowing scattering particles to access the previously forbidden region. Scattering then becomes chaotic for $E > E_c$. The key difference between this scenario to chaotic scattering and the previously studied one [9] is that in the present route, there is a *discontinuous* change in the fractal dimension of the set of singularities in the scattering function due to the sudden access of scattering particles to an already developed chaotic set. In what follows, we choose a class of potential functions to demonstrate how naturally this abrupt bifurcation to chaotic scattering can occur in physically realistic situations. We then analyze the basic dynamical characteristics of the bifurcation.

To construct a model, we consider physical situations where particles are scattered off by molecules. Assume that there are three molecules located at the vertices (x_j, y_j) ($j = 1, 2, 3$) of a triangle of equal length in the plane. For each molecule, its interaction with a scattering particle can be

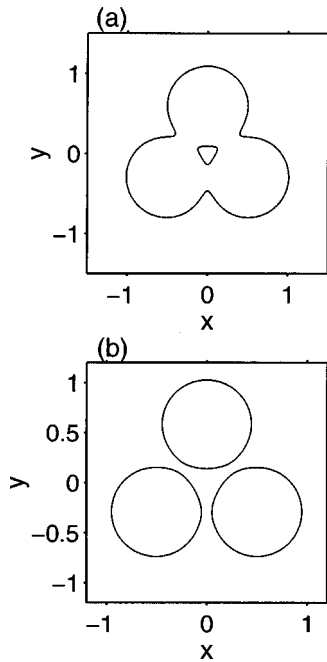


FIG. 1. Contour plots of the Morse potential configuration: (a) $E=1$, and (b) $E=4$.

modeled by the Morse potential [13], which has been a paradigm for studying various phenomena in chemical and atomic physics [14]. The dimensionless potential function of our scattering system can then be written as

$$V(x,y) = \frac{V_0}{2} \sum_{j=1}^3 [1 - e^{-\alpha(r_j - r_e)}]^2, \quad (1)$$

where $r_j = \sqrt{(x-x_j)^2 + (y-y_j)^2}$ ($j=1,2,3$), and V_0 , α , and r_e are parameters of the Morse potential. Due to conservation of energy, the phase-space dimension is three. In our numerical experiments, we fix the following set of parameter values $m=1$, $V_0=1$, $\alpha=6$, and $r_e=0.68$. The locations of the vertices of the triangle are $(x_1, y_1) = (1/2, -1/(2\sqrt{3}))$, $(x_2, y_2) = (-1/2, -1/(2\sqrt{3}))$, and $(x_3, y_3) = (0, \sqrt{1/3})$. The Hamilton's equations of motion are integrated by using the standard Störmer-Verlet method, which preserves the symplecticity of the system [15]. The potential distribution is highly localized and we denote the region around $(x,y) = (0,0)$, where $V(x,y)$ is appreciable, the *scattering region*. The difference between our scattering model and the previously studied one [9] is that our potential function is more realistic and the height of the potential is large so that in a practical sense, the potential hills are classically impenetrable. As such, the abrupt bifurcation in our system occurs at low energies when the energy is increased through a critical value, in contrast to the case treated in Ref. [9] where the bifurcation occurs at high energies when the particle energy is *decreased* through a critical value.

We focus on the physically realistic energy regime where the particle energy is much smaller than the height of the potential hills: $E \ll V(x_j, y_j)$ ($j=1,2,3$). Figures 1(a) and 2(b) show the contours of the potential for $E=1$ and for $E=4$, respectively, where for $E=1$, the region enclosed between the inner and outer closed curves is the classically

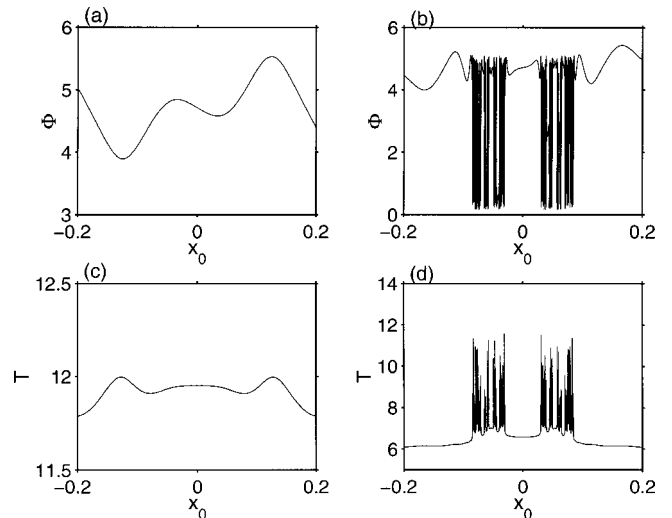


FIG. 2. (a) and (b): Scattering functions $\phi(x_0)$ for $E=1$, and $E=4$, respectively. (c) and (d): Delay-time functions $T(x_0)$ for $E=1$, and $E=4$, respectively.

forbidden one, and for $E=4$, the regions enclosed by three circularlike curves are the classically forbidden regions. Thus, for $E=1$, particles coming from far away cannot enter the scattering region and are simply bounced back from the potential. In this case, the scattering is regular. However, for $E=4$, the potential configuration is similar to that of three hard disks [16] for which the scattering is chaotic. Figures 2(a) and 2(b) show the scattering functions for $E=1$ and $E=4$, respectively, where the outgoing angle $\phi \equiv \tan^{-1}(p_y/p_x)$ of the particle trajectory after the scattering (p_x and p_y are the x and y components of the momentum) is plotted against the impact parameter x_0 . To make these plots, 5000 particles uniformly distributed in the interval $x_0 \in [-0.2, 0.2]$ at $y_0 = -8$ are launched upwards in the $+y$ direction, and the scattering variable ϕ is recorded when the particles exit the scattering region, say, when $r = \sqrt{x^2 + y^2} \geq 10$. We see that scattering is regular for $E=1$ because the scattering function is smooth, while for $E=4$, the scattering becomes chaotic as there appears to be an infinite number of singularities in the scattering function. Figures 2(c) and 2(d) show the corresponding delay-time plots for $E=1$ and $E=4$, respectively, where T is the time that a particle spends in the scattering region before exiting it.

The absence and presence of chaotic scattering at $E=1$ and $E=4$, respectively, suggest that there is a bifurcation to chaotic scattering as E is increased from 1 to 4. Here we argue that this bifurcation is abrupt. Note that at $E=1$, there is a triangularlike area in the center of the scattering region [Fig. 1(a)] in which the value of the potential is actually lower than E and, hence, this area is classically allowed for particle trajectories. This region, however, is *inaccessible* to scattering particles from outside because it is surrounded by a larger classically forbidden region. Dynamics inside the triangularlike potential region can be chaotic. In fact, we find that for $E=1$, the corresponding phase space contains both Kol'mogorov-Arnol'd Moser (KAM) tori and Hamiltonian chaotic seas, as shown in Fig. 3(a), where the x coordinate and its momentum of particle trajectories are plotted on the Poincaré surface of section defined by $y=0$. Chaos in this

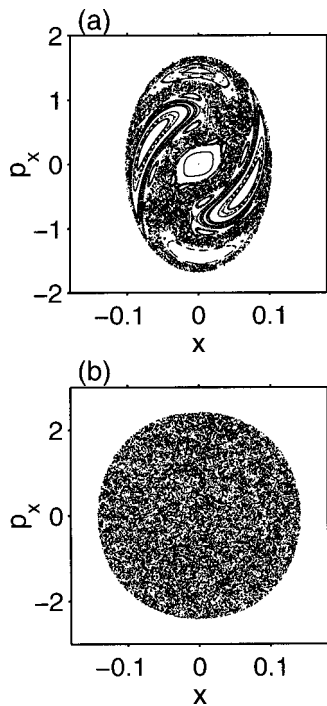


FIG. 3. Phase-space structure on Poincaré surface of section of the classically allowed region that is inaccessible to scattering particles for: (a) $E=1$, and (b) $E=2.5 < E_c$. There are both KAM surfaces and bounded chaotic sea for $E=1$. For $E=2.5$, all KAM surfaces have apparently disappeared.

case is bounded. As E is increased, the triangularlike area enlarges and the phase-space structure inside also evolves. In particular, KAM tori are destroyed and the chaotic sea is enlarged, as shown by the phase-space structure on the Poincaré surface of section in Fig. 3(b) for $E=2.5$. At some critical energy value E_c where the inner classically allowed region connects with the outside one, the previously bounded chaotic sea becomes transient because trajectories can escape through one of the openings. Now, particles coming from outside can get access to the transient chaotic region so that the scattering becomes chaotic. The appearance of chaotic scattering is abrupt because for $E < E_c$, the scattering dynamics is smooth, while it is chaotic for $E > E_c$. Numerically, for the scattering configuration described, we find $E_c \approx 2.55$.

Depending on whether there are still KAM tori left for $E \geq E_c$, the chaotic scattering can be either hyperbolic or nonhyperbolic. In hyperbolic chaotic scattering, all the periodic orbits are unstable and there are no KAM surfaces in the scattering region. A characteristic feature of hyperbolic chaotic scattering is that the survival probability of a particle in the scattering region decays exponentially with time: $P(t) \sim e^{-\gamma t}$, where t is time and $\tau=1/\gamma$ is the lifetime of the chaotic saddle [11]. On the other hand, in nonhyperbolic chaotic scattering, there are both KAM surfaces and chaotic regions in the phase space [17,18]. Due to the ‘‘stickiness’’ of KAM surfaces, the survival probability of a scattering particle decays algebraically with time [19]: $P(t) \sim t^{-z}$ for large t . In the present route to chaotic scattering, depending on whether there are still KAM tori left for $E \geq E_c$, the scattering can be either hyperbolic or nonhyperbolic. Numerically, we find that for the scattering configuration described,

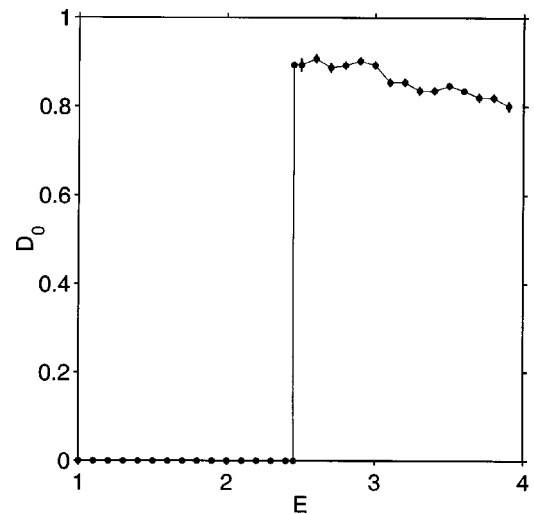


FIG. 4. Fractal dimension D_0 of the set of singularities in the scattering function vs E . There is a discontinuous change in D_0 at E_c , the abrupt bifurcation point to chaotic scattering.

abrupt bifurcation leads to *hyperbolic chaotic scattering*. An alteration in the scattering configuration can easily lead to abrupt bifurcation to nonhyperbolic chaotic scattering. For instance, when the Morse molecule on the y axis is pulled closer to the pair in the x direction, say at $y_3=0.45$, there are still KAM surfaces left in the scattering region after the bifurcation that connects the inner and outside classically allowed regions.

The major *physically measurable* consequence of the abrupt bifurcation to chaotic scattering described above is that there is a discontinuous change in the fractal dimension D_0 of the set of singularities in the scattering function. From Figs. 2(a)–2(d) it is apparent that for $E < E_c$ (before the bifurcation), both the scattering and the delay-time functions are smooth, and, hence, $D_0=0$. For $E > E_c$ (after the bifurcation), the scattering and the delay-time functions suddenly contain a Cantor set of singularities with $D_0 > 0$. To compute the values of D_0 , we use the uncertainty algorithm [20]. Specifically, we randomly choose a large number of pairs of particles with distance ϵ apart from a line segment at $y_0 = -10$ and compute, for each pair, whether the two particles exit the scattering region through different open channels shown in Fig. 1(b). The fraction of these uncertain pairs $f(\epsilon)$ typically scales with ϵ as $f(\epsilon) \sim \epsilon^{1-D_0}$ [20]. In the actual computation, for each energy value, $f(\epsilon)$ is approximated by N_u/N_0 , where N_u is the number of uncertain pairs among N_0 pairs of initial conditions chosen (we fix $N_u=200$). Figure 4 shows D_0 versus E for $1.0 \leq E \leq 4.0$, where the sudden jump in D_0 at E_c is apparent. Theoretically, for E immediately above E_c when the bounded chaotic sea in the scattering region just becomes transient, the value of D_0 is unity because by continuity, the box-counting dimension of the chaotic saddle for $E \geq E_c$ is the same as that of the Hamiltonian chaotic sea for $E \leq E_c$, which is the phase-space dimension. Numerically, we find that $D_0 \approx 0.9$ for $E=2.6 > E_c$. On the other hand, the jump in D_0 will be unity at the abrupt bifurcation if it leads to nonhyperbolic chaotic scattering, although it is unlikely to obtain $D_0=1$ in numerical computations [21]. We note that this discontinuous change in the fractal dimension is the key ingredient that distinguishes our

abrupt route to chaotic scattering from the previously studied one [9]: in that case the dimension scales with E inversely logarithmically and the dimension is in fact continuous at the bifurcation.

In summary, we analyzed an alternate type of abrupt bifurcation to chaotic scattering. The bifurcation occurs when a closed Hamiltonian chaotic sea, hyperbolic or nonhyperbolic, suddenly becomes accessible to scattering trajectories as a system parameter changes. Consequently, there is a dis-

continuous increase in the fractal dimension of the set of singularities in the scattering function. We expect this bifurcation to be observable because the model that we have utilized to illustrate this bifurcation is constructed in a physically realistic way.

This work was supported by AFOSR under Grant No. F49620-98-1-0400 and by NSF under Grant No. PHY-9722156.

-
- [1] For example, M. C. Gutzwiller, *Physica D* **7**, 341 (1983); C. Jung, *J. Phys. A* **19**, 1345 (1986); M. Hénon, *Icarus* **66**, 536 (1986); *Physica D* **33**, 132 (1998); B. Eckhardt, *Europhys. Lett.* **61**, 329 (1988); G. Troland U. Smilansky, *Physica D* **35**, 34 (1989); Z. Kovács and T. Tél, *Phys. Rev. Lett.* **64**, 1617 (1990); Y.-C. Lai and C. Grebogi, *Phys. Rev. E* **49**, 3761 (1994).
- [2] T. Tél and E. Oh, *Chaos (Focus Issue)* **3**, 417 (1993).
- [3] See, for example, R. Blümel, *Chaos* **3**, 683 (1993).
- [4] See, for example, P. T. Boyd and S. L. W. McMillian, *Chaos* **3**, 507 (1993).
- [5] See, for example, B. Eckhardt and H. Aref, *Trans. Soc. R. London A* **326**, 655 (1988); E. Ziemniak, C. Jung, T. Tél, *Physica D* **76**, 123 (1994); A. Péntek, T. Tél, and Z. Toroczkai, *J. Phys. A* **28**, 2191 (1995).
- [6] See, for example, D. W. Noid, S. Gray, and S. A. Rice, *J. Chem. Phys.* **84**, 2649 (1986); Z. Kovács and L. Wiesenfeld, *Phys. Rev. E* **51**, 5476 (1995).
- [7] See, for example, R. A. Jalabert, H. U. Baranger, and A. D. Stone, *Phys. Rev. Lett.* **65**, 2442 (1990); C. M. Marcus, R. M. Westervelt, P. F. Hopkins, and A. C. Gossard, *Chaos* **3**, 643 (1993).
- [8] N. J. Cornish and E. P. S. Shellard, *Phys. Rev. Lett.* **81**, 3571 (1998).
- [9] S. Bleher, C. Grebogi, and E. Ott, *Physica D* **46**, 87 (1990).
- [10] C. Grebogi, E. Ott, and J. A. Yorke, *Physica D* **7**, 181 (1983).
- [11] T. Tél, in *Directions in Chaos*, edited by Bai-lin Hao (World Scientific, Singapore, 1990), Vol.3; in *STATPHYS 19*, edited by Bai-lin Hao (World Scientific, Singapore, 1996).
- [12] H. Kantz and P. Grassberger, *Physica D* **17**, 75 (1985).
- [13] P. M. Morse, *Phys. Rev.* **34**, 57 (1929); D. ter Haar, *ibid.* **70**, 222 (1946);
- [14] See, for example, J. Heagy and J. M. Yuan, *Phys. Rev. A* **41**, 571 (1990), and references therein.
- [15] L. Verlet *Phys. Rev.* **159**, 98 (1967).
- [16] P. Gaspard and S. A. Rice, *J. Chem. Phys.* **90**, 2225 (1989).
- [17] M. Ding, C. Grebogi, E. Ott, and J. A. Yorke, *Phys. Rev. A* **42**, 7025 (1990).
- [18] Y.-C. Lai, R. Blümel, E. Ott, and C. Grebogi, *Phys. Rev. Lett.* **68**, 3491 (1992); Y.-C. Lai, M. Ding, C. Grebogi, and R. Blümel, *Phys. Rev. A* **46**, 4661 (1992).
- [19] J. D. Meiss, J. R. Cary, C. Grebogi, C. Grebogi, J. D. Crawford, A. N. Kaufman, and H. D. I. Abarbanel, *Physica D* **6**, 375 (1983); C. F. F. Karney, *ibid.* **8**, 360 (1983); B. V. Chirikov and D. L. Shepelyansky *ibid.* **13**, 395 (1984); J. D. Meiss and E. Ott, *Phys. Rev. Lett.* **55**, 2741 (1985).
- [20] S. W. McDonald, C. Grebogi, E. Ott, and J. A. Yorke, *Physica D* **17**, 125 (1985).
- [21] Y. T. Lau, J. M. Finn, and E. Ott, *Phys. Rev. Lett.* **66**, 978 (1991).